IAEA FUMAC BENCHMARK ON THE UNCERTAINTY AND SENSITIVITY ANALYSIS FOR FUEL ROD CODE SIMULATION OF THE HALDEN LOCA TEST IFA-650.10

JINZHAO ZHANG*
Tractebel (ENGIE), Boulvard Simon Bolivar 34-36, 1000 Brussels, Belgium
**Corresponding author: +32 2 773 9843, jinzhao.zhang@tractebel.engie.com*

ANTOINE BOULORÉ
CEA/DEN/Cadarache, Fuel Research Department
13108 Saint-Paul-lez-Durance, FRANCE

ABSTRACT

In framework of the IAEA FUel Modelling in Accident Conditions (FUMAC) project, an uncertainty and sensitivity analysis benchmark has been performed on the simulation of the Halden LOCA test IFA-650.10 using different fuel rod codes. This paper describes the used fuel rod codes and statistical uncertainty and sensitivity analysis tools, the Halden LOCA test IFA-650.10, the specifications for the uncertainty and sensitivity analysis, and the comparison and discussion of the uncertainty and sensitivity analysis results provided by the participants.

1. Introduction

The FUMAC (Fuel Modelling in Accident Conditions) project has been launched by IAEA as a new Co-ordinated Research Project (CRP) in 2014-2018 [1]. It is a continuation of the previous FUMEX III project [2] with the focus on the modelling of fuel behaviours in design basis and severe accidents, in particular, Loss-Of-Coolant Accidents (LOCAs).

Within framework of the FUMAC project, an uncertainty and sensitivity analysis (UASA) was performed on the modelling of the Halden LOCA test IFA-650.10 (PWR rod, without significant axial relocation) [3] with different fuel rod codes. The objective is to verify if the quantified uncertainties on the predicted uncertainty bands of the key physical parameters (clad and fuel temperature, rod internal pressure, clad elongation, and clad outside diameter) well bound the measured data during the test, and as an optional activity for the interested participants, to identify the most influential input uncertainty parameters through global sensitivity analysis (GSA). Detailed specifications have been provided.

This paper describes the used fuel rod codes and statistical uncertainty and sensitivity analysis tools (§2), the Halden LOCA test IFA-650.10 (§3), the specifications for the uncertainty and sensitivity analysis (§4), and the comparison and discussion of the uncertainty and sensitivity analysis results provided by the participants (§5).

2. Participants and used codes

As shown in the following Tab 1, seven participants have performed the uncertainty analysis, and six participants have performed the sensitivity analysis.

Five different fuel rod codes (DIONISIO, ALCYONE, FTPAC, FRAPTRAN, TRANSURANUS) and four different statistical uncertainty and sensitivity analysis tools (DAKOTA, URANIE, Excel, and built-in Monte Carlo function) were used.

Participant	Code	UA/SA Tool	UA	SA
CNEA	DIONISIO-2.0	DAKOTA	Y	Y
CEA	ALCYONE-1D	URANIE	Y	Y
CIAE	FTPAC	DAKOTA	Y	Y
CIEMAT	FRAPTRAN-1.5	DAKOTA	Y	Y
IPEN	FRAPTRAN	Excel	Y	Y
Tractebel	FRAPTRAN-TE-1.5	DAKOTA	Y	Y
JRC	TRANSURANUS	Built-in (M-C)	Y	

Tab 1: Participants to uncertainty and sensitivity analysis.

The analyses were performed according to the specifications, and the requested results were provided. The submitted main results of the participants will be analysed and discussed, in comparison with the available experimental data.

3. The Halden LOCA test IFA-650.10

3.1 Test rig and rod instrumentations

The objective of the Halden LOCA tests IFA-650 is to study fuel behaviours such as fuel fragmentation and relocation, cladding ballooning, burst (rupture) and oxidation during typical LOCA transient for PWR, BWR and VVER high burnup fuels. In the IFA-650 LOCA tests, a single fuel rodlet is located in a high-pressure flask connected to the heavy water loop 13 of the Halden reactor. The fuel power is controlled by reactor power. Nuclear power generation in the fuel rodlet is used to simulate decay heat, whereas the electrical heater surrounding the rod is simulating the heat from surrounding rods.

As shown in Fig. 1, the rig and rod instrumentations consisted of three cladding thermocouples at the bottom (TCC1) and upper (TCC2 & 3) part of the rod, three heater thermocouples at different axial elevations (TCH1 at bottom, TCH2 at mid and TCH3 at top), a cladding extensometer (EC2) and a rod pressure sensor (PF1), rig coolant thermocouples (two at rig inlet, TI, and two at outlet, TO), and three axially distributed vanadium neutron detectors (ND) to measure the axial power distribution.

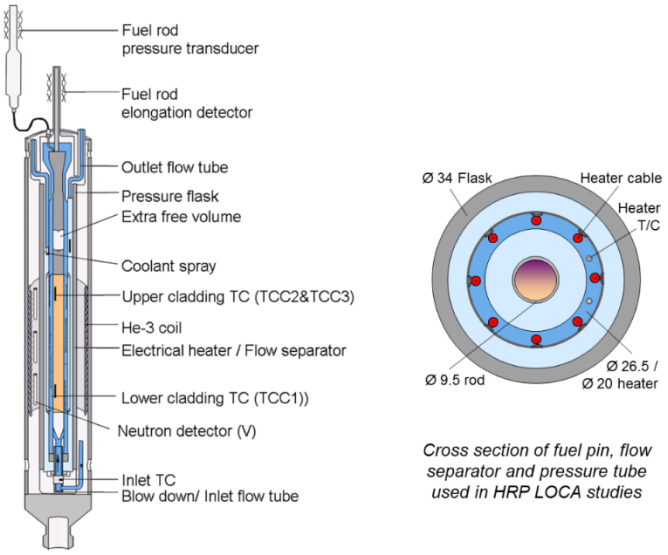

Fig 1. Halden LOCA high pressure flask for IFA-650 tests [3].

3.2 IFA650.10 test

The detailed description of IFA-650.10 test can be found in [3]. The test segment was cut from a standard PWR fuel rod test which had been irradiated in the PWR Gravelines 5 (900 MWe EDF, France) during five cycles from August 1988 to August 1995 to a burn-up of 61

MWd/kgU (average cycle powers 195, 230, 215, 185 and 150 W/cm). The length of the fuel stack was ~ 440 mm and no end pellets were inserted.

The rod was filled with a gas mixture of 95 % argon and 5 % helium at 40 bar. Argon was chosen to simulate the fission gases, whereas a small amount of helium is required for the leak test of the rod. The rod plenum volume (free gas volume) was made relatively large in order to maintain stable pressure conditions until cladding burst. The total free gas volume of ~16-17 cm³ was thus practically all located in the plenum, outside the heated region.

The test was conducted in May 2010. The evolution of the main test results is illustrated in Fig 2.

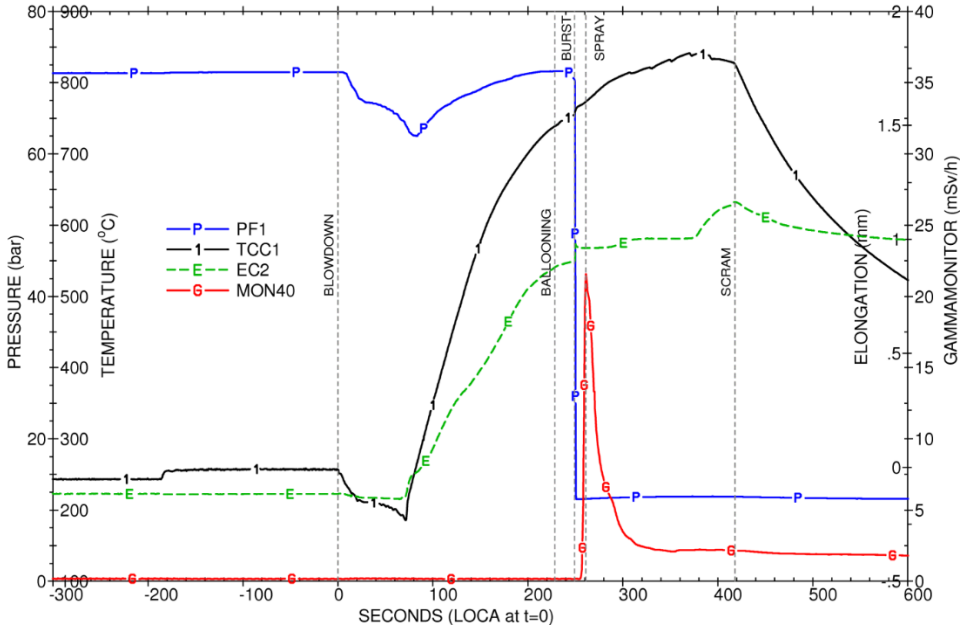

Fig 2. Evolution of the main test results for IFA-650.10 [3].

The initial loop pressure was ~70 bar and the counter pressure in the blowdown tank was ~2 bar. Shortly before the test start, the outer loop was by-passed, and after ~3 minutes with natural circulation in the rig, the LOCA was initiated by opening the valves leading to the shielded blowdown tank. The target peak cladding temperature was 850 °C. Cladding failure occurred ~249 s after blowdown at ~755 °C (TCC1) as evidenced by pressure, cladding temperature measurements as well as the gamma monitor on the blowdown line to the dump tank. Spraying was started 12 s after the burst in order to ensure that the fission products are transported out of the loop. The test was terminated by a reactor scram 418 s after the blowdown initiation. At the end of the test, the rig was filled with helium for dry storage.

Slight clad ballooning and burst were detected in-pile and verified by the gamma scanning performed at Halden. No fuel relocation was seen during the test, which was subsequently confirmed by the gamma scanning.

4. Specifications for the uncertainty and sensitivity analysis

4.1 Uncertainty and sensitivity analysis method

Among all the available uncertainty analysis methods, the probabilistic input uncertainty propagation method is, so-far, the most widely used in nuclear safety analysis [4]. In this method, the fuel codes are treated as “black boxes”, and the input uncertainties are propagated to the simulation model output uncertainties via the code calculations, with sampled data from known or assumed distributions for key input parameters. The input parameters of interest may also include uncertain material properties, model parameters, etc.

The method consists in the following steps:

1) Identification of input uncertainties: All relevant code outputs and corresponding uncertain parameters for the codes, plant modelling schemes, and plant operating conditions are identified.

2) Definition of input uncertainties: the uncertainty of each uncertain parameter is quantified by a probability density function (PDF) based on engineering judgment and experience feedback from code applications to separate and integral effect tests and to full plants simulation. The PDF can also be based on experimental data if available. If dependencies between uncertain parameters are known and judged to be potentially important, they can be quantified by correlation coefficients.

3) Propagation of uncertainties through the computer code: the propagation is represented by Monte-Carlo simulations. In Monte-Carlo simulations, the computer code is run repeatedly, each time using different values for each of the uncertain parameters. These values are drawn from the probability distributions and dependencies chosen in the previous step. In this way, one value for each uncertain parameter is sampled simultaneously in each repetition of the simulation. The results of a Monte-Carlo simulation lead to a sample of the same size for each output quantity.

4) Statistical analysis of the results: the output sample is used to get any typical statistics of the code response such as mean or variance and to determine the cumulative distribution function (CDF). The CDF allows deriving the percentiles of the distribution.

The probabilistic input uncertainty propagation method is selected due to its simplicity, robustness and transparency. The highly recommended sample size is set to 200 (i.e. 200 code runs must be performed). The sample is constructed according to the selected PDFs coming from the uncertainty modelling step and assuming independence between input parameters following a Simple Random Sampling (SRS). A lower and upper uncertainty bound of the 5% and 95% percentiles at confidence level higher than 95 % are estimated by the 196^{th} and 5^{th} rank, respectively, by using the order statistics method [5]-[8].

Besides statistical uncertainty analysis, a global sensitivity analysis is also performed to get qualitative insights on the most influential input parameters, using the previously obtained 200 code runs. The identification is based on various sensitivity indices and significance thresholds [9]-[11].

4.2 Specifications of input uncertainties

Detailed specifications have been made for input uncertainty parameters and their distributions, as shown in Tab 2.
For each input uncertainty parameter, the information includes a mean value, a standard deviation and a type of distribution. In order to avoid unphysical numerical values, a range of variation (lower and upper bounds) is also provided. The sampling is performed between the upper and lower bounds, i.e. the PDFs are truncated. In order to simplify the current benchmark application, a normal distribution is assigned to all the considered input parameters. Their standard deviation is taken as the half of the maximum of the absolute value of the difference between their nominal value and their upper or lower bound for all input parameters.

Input uncertainty parameter	Distribution				
	Mean	Standard Deviation	Type	Lower bound	Upper bound
Cladding outside diameter (mm)	9.50	0.01	Normal	9.48	9.52
Cladding inside diameter (mm)	8.36	0.01	Normal	8.34	8.38
Pellet outside diameter	8.2	0.01	Normal	8.18	8.22
Fuel theoretical density (kg/m3 at 20 °C)	10457	50	Normal	10357	10557
U235 enrichment (%)	4.487	0.05	Normal	4.387	4.587
Filling gas pressure (MPa)	4.0	0.05	Normal	3.9	4.1
Relative power during base irradiation	1	0.01	Normal	0.98	1.02
Relative power during test	1	0.025	Normal	0.95	1.05
Test rod power profile	1	0.01	Normal	0.98	1.02
Code calculated coolant temperature (°C)	1	5	-	T-10	T+10
Code calculated clad-to-coolant heat transfer coefficient ($W/m^2.°C$)	1	0.125	Normal	0.75	1.25
Fuel thermal conductivity model	1.00	5%	Normal	0.90	1.10
Clad thermal conductivity model	1.00	5%	Normal	0.90	1.10
Fuel thermal expansion model	1.00	5%	Normal	0.90	1.10
Clad thermal expansion model	1.00	5%	Normal	0.90	1.10
Fuel densification model	1.00	5%	Normal	0.90	1.10
Fuel solid swelling model	1.00	5%	Normal	0.90	1.10
Fuel gaseous swelling model	1.00	5%	Normal	0.90	1.10
Clad Yield stress	1.05	5%	Normal	0.95	1.15
Fuel heat capacity	1.00	1.5%	Normal	0.97	1.03
Cladding heat capacity	1.00	1.5%	Normal	0.97	1.03
Cladding elastic modulus	1.00	5%	Normal	0.90	1.10
Cladding corrosion model during steady-state operation	1.00	12.5%	Normal	0.75	1.25
Cladding hydrogen pickup fraction during steady-state operation	1.00	15%	Normal	0.7	1.30
Cladding oxidation model at high temperature	1.00	15%	Normal	0.7	1.30
Thermal conductivity of the oxide layer	1.00	10%	Normal	0.80	1.20
Fission gas release (or gas diffusion coefficient)	1.00	25%	Normal	0.50	1.50
Gap gas conductivity	1.00	12.5%	Normal	0.75	1.25
Fuel/cladding emissivity	1.00	5%	Normal	0.90	1.10
Fuel radial relocation	1.00	10%	Normal	0.80	1.20
Fuel fragment packing fraction (if applicable)	0.72	10%	Normal	0.58	0.86
Cladding strain threshold for fuel mobility (if applicable)	1.00	10%	Normal	0.80	1.20
Cladding Meyer hardness	1.00	5%	Normal	0.90	1.10
Cladding annealing	0.15	5%	Normal	0.05	0.25
Cladding burst criteria	1.00	10%	Normal	0.80	1.20
Cladding burst strain criteria	1.00	10%	Normal	0.80	1.20
Plenum gas temperature [°C]	-	5	-	T-10	T+10

Tab 2: Specification of the input uncertainty parameters for IFA-650.10.

The effect of the uncertainty modelling (i.e. the choice of a normal distribution and the correlation between input parameters) is not studied in this work. Although this effect could have some impact on the derived uncertainty bands, the conclusions of this exercise are expected to be similar for other distributions.

All the runs of the code have to be completed (no code crash), otherwise the determination of the quantiles and of the sensitivity indices would be biased.

5. Results and discussion

5.1 Uncertainty analysis results

The calculation results of the 200 successful runs are collected, and the 5th and 196th ranks are chosen to estimate the upper/lower (95%/5%) uncertainty bounds (LB, UB) of the output parameter of interest, according to the order statistics (except that JRC used directly Monte Carlo method to obtain the upper/lower (95%/5%) uncertainty bounds (LB, UB)). The results of the reference case (REF) are also provided.

Comparison of the value of the available experimental data within the reference and upper bound values by different participants for each of the main output parameters allows an assessment of the adequacy of the model and the conservatism of the upper bound value. An example of such comparison for rod internal pressure (RIP) upper bound value is shown in Fig 3. The calculated upper bound rod internal pressure by each participant does not bound the experimental data, except for Tractebel (trend and burst time) and JRC (burst time). It is worthwhile to note the difference of results between CIEMAT, IPEN and Tractebel, using the same FRAPTRAN code but with different versions and options, as well as different assumptions (clad temperature and plenum gas temperature). The difference is mainly due to the differences in the plenum gas temperature modelling.

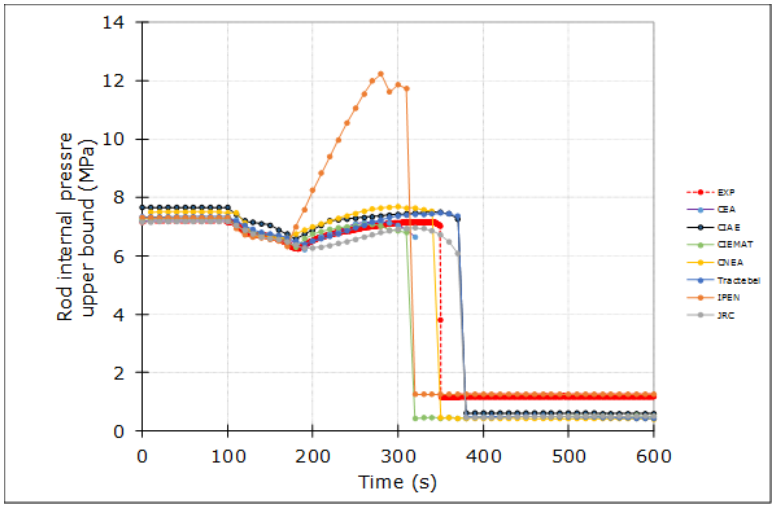

Fig 3. Comparison of the upper bound values for rod internal pressure (RIP).

Comparison of the uncertainty bands obtained by different participants for each of the main output parameters with measurement allows to quantify the *accuracy* of the model. Comparison of the position of the reference case within the uncertainty bands by different participants for each of the main out parameters allows detection of *bias* (if any) in the model. An example of such comparison for clad outer surface temperature (TCO) uncertainty bands is shown in Fig 4. The uncertainty bounds are between 0-80 °C, which is about 10% of the reference value. In general, the uncertainty bands are higher after burst. It is worthwhile to note the difference of results between CIEMAT, IPEN and Tractebel, using the same FRAPTRAN code but with different versions and options, as well as different assumptions. The difference can be attributed to the different assumptions used: for example, some participants (IPEN) directly used the measured clad temperature, instead of using the code

calculated coolant temperature and heat transfer coefficient and considering the associated uncertainties as requested in the Specifications (see Tab 2).

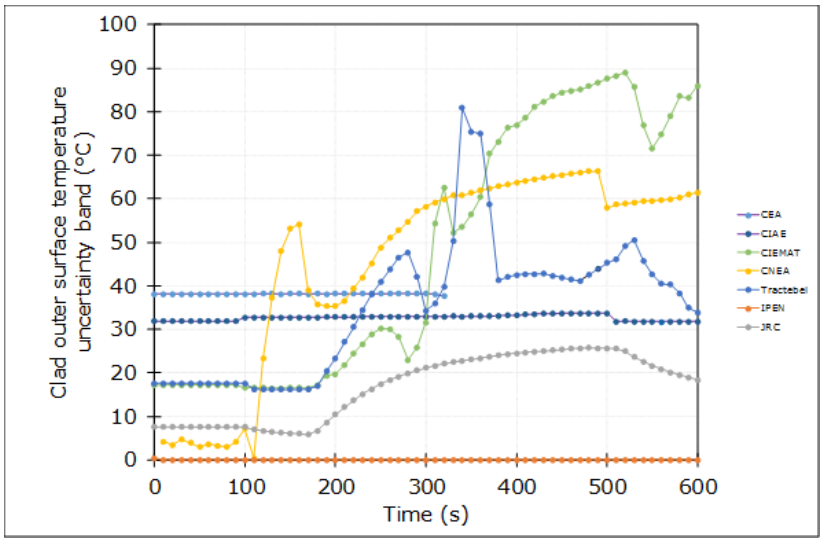

Fig 4. Comparison of the uncertainty bands for clad outer surface temperature (TCO).

Finally, comparison of the global difference between the maximum UB values and minimum LB values (global uncertainty width) and total difference between the maximum REF values and minimum REF values (global reference dispersion) allows identification of the proportion of the model difference in the global uncertainty width, as well as the position of the experimental data. An example of such comparison for rod internal pressure (RIP) is shown in Fig 5. The experimental data are bounded by both the minimum and maximum reference values (reference dispersion) of all participants' results and the minimum LB values and maximum UB values (uncertainty width). This indicates that there is no bias in the rod internal pressure model, whose uncertainty band can be quantified by the statistical approach.

A different situation can be observed on Fig 6 for the clad outer surface temperature (TCO). Both the minimum of LB and reference values of the outer surface temperature are close to the experimental data, indicating significant bias in the thermal hydraulic boundary conditions (albeit the requirements of using the same thermal hydraulic boundary conditions in the Specifications).

A much large dispersion can be observed on Fig 7 & 8 for clad total elongation (ECT) and clad outside diameter (DCO) at burst node, respectively. This indicates that the difference between the reference values of all participants are dominant in the global uncertainty width. The maximum UB and REF values for ECT (Fig 7) and the minimum LB and REF values for DCO (Fig 8) are quite close, indicating that the mechanical models have significant bias and is not adequate for uncertainty analysis before further improvement.

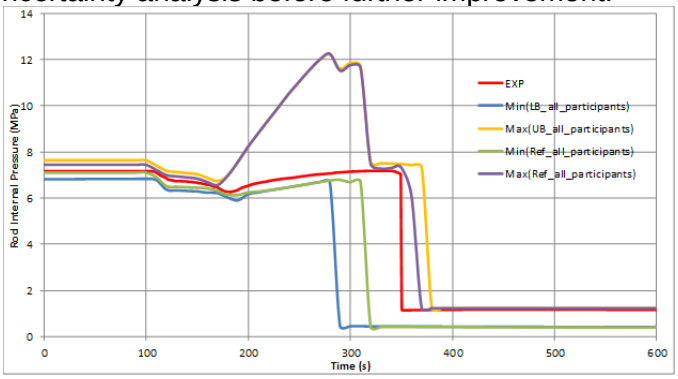

Fig 5. The global reference dispersion and uncertainty width of all participants for rod internal pressure (RIP).

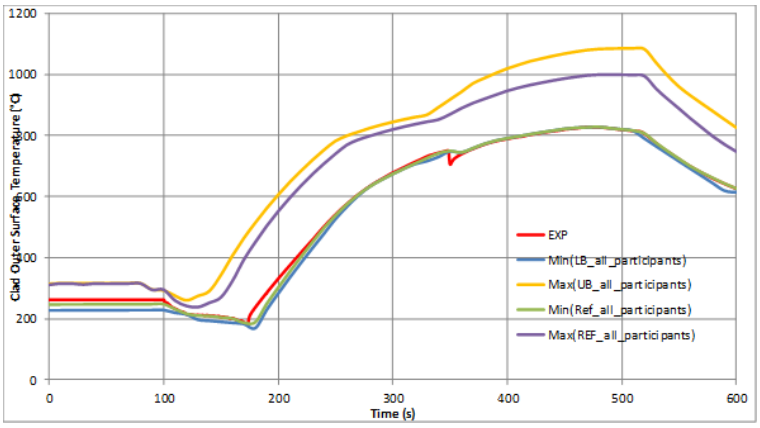

Fig 6. The global reference dispersion and uncertainty width of all participants for clad outer surface temperature (TCO).

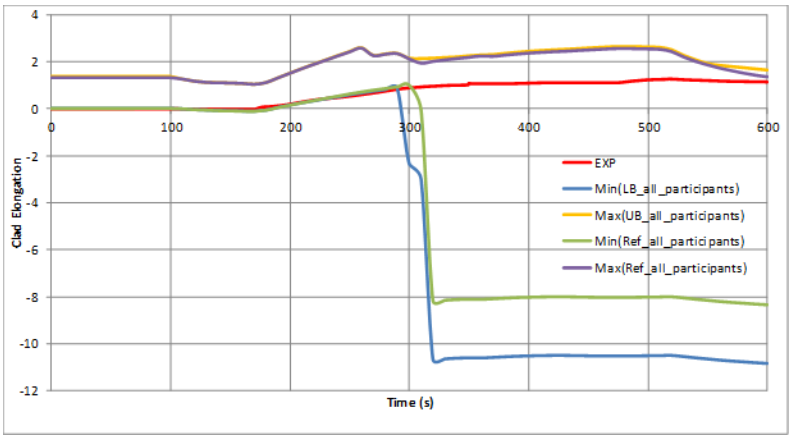

Fig 7. The global reference dispersion and uncertainty width of all participants for clad total elongation (ECT).

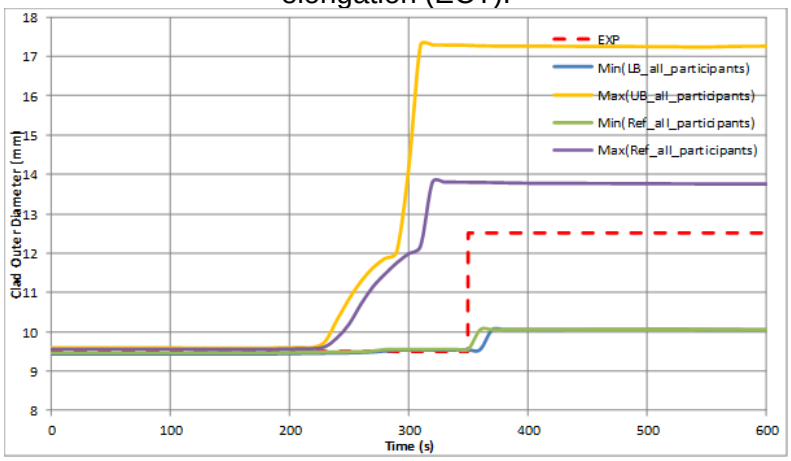

Fig 8. The global reference dispersion and uncertainty width of all participants for clad outside diameter (DCO) at burst node.

5.2 Sensitivity analysis results

The global sensitivity analysis (GSA) is a powerful tool to identify the most influential input uncertainty parameters on each output parameter of interest. They can be identified by using various sensitivity indices like correlation coefficients and well-defined significance thresholds. Specific guidance and interpretation of the significance depends on the number of samples, number of variables, and analysis tolerance [9]-[11].

As the fuel rod codes have very complex models, and there are certain interactions between input parameters, the correlation coefficients can only be considered as qualitative and relative index for screening the non-influential input parameters.

In the current work, the Partial Rank Correlation Coefficients (PRCCs) are used and arbitrary significance threshold of 0.5 are chosen for identification of the high influence of the input uncertainty parameters on the output parameter (i.e., PRCC > 0.5). Lower values imply low (PRCC < 0.25) or medium influence (0.25 ≤PRCC≤0.5). An example of the calculated PRCCs by Tractebel, using FRAPTRAN-TE-1.5 and DAKOTA, is shown in Tab 3.

The PRCCs for each output parameter of interest as a function of all the input parameters change during the transient and with each code. The values shown in this table are the maximum during the transient. The red cells are those of high influence (PRCC > 0.5) at least at 1 of the instant during the transient.

Comparison of the PRCCs by different participants for each of the main output parameters allows the identification of a common list of high influential input data or models. It would be also interesting to do so for a group of parameters in order to identify high influential input data or models for all aspects (Fuel thermal, clad thermal, mechanical, overall) of the fuel rod code.

Based on the current sensitivity study results, the common list of high influential input uncertainty parameters can be identified for each aspect of the fuel rod code, as shown in the following Tab 4. The red cells with “1” means high influence identified for at least 1 output parameter for that aspect.

Input uncertainty parameter	RIP	TFC	TFO	TCI	TCO	TOL	ECR	DCO	CES	ECT	EFT
Cladding outside diameter (mm)	18%	9%	12%	13%	12%	11%	83%	19%	83%	17%	8%
Cladding inside diameter (mm)	70%	65%	64%	50%	50%	6%	82%	81%	90%	79%	50%
Pellet outside diameter	65%	56%	60%	40%	40%	7%	17%	88%	77%	79%	48%
Fuel theoretical density (kg/m3 at 20 °C)	10%	39%	36%	38%	38%	9%	9%	13%	10%	15%	21%
U235 enrichment (%)	10%	10%	12%	12%	12%	9%	8%	11%	12%	11%	14%
Filling gas pressure (MPa)	98%	15%	30%	28%	28%	8%	17%	35%	92%	26%	11%
Relative power during base irradiation	10%	8%	9%	9%	9%	6%	10%	7%	8%	10%	9%
Relative power during test	53%	94%	93%	94%	94%	52%	54%	80%	33%	39%	84%
Test rod power profile	10%	25%	7%	8%	7%	11%	8%	85%	9%	10%	6%
Cladding temperature (°C)											
Coolant temperature (°C)	39%	86%	96%	100%	100%	58%	60%	78%	27%	87%	90%
Clad-to-Coolant heat transfer coefficient	85%	100%	98%	99%	99%	90%	91%	96%	64%	77%	94%
Fuel thermal conductivity model	16%	80%	28%	28%	28%	14%	15%	10%	7%	44%	42%
Clad thermal conductivity model	11%	9%	8%	44%	8%	9%	8%	7%	5%	9%	4%
Fuel thermal expansion model	18%	19%	17%	13%	13%	8%	17%	51%	43%	61%	89%
Clad thermal expansion model	11%	11%	12%	14%	15%	7%	6%	96%	19%	97%	9%
Fuel densification model	24%	36%	38%	18%	18%	7%	10%	61%	51%	54%	35%
Fuel solid swelling model	23%	40%	41%	24%	24%	11%	16%	62%	55%	60%	31%
Fuel gaseous swelling model	39%	38%	38%	24%	24%	10%	11%	65%	56%	61%	30%
Clad Yield stress	44%	25%	59%	67%	66%	15%	37%	77%	36%	55%	21%
Fuel heat capacity	20%	69%	67%	69%	69%	14%	13%	31%	16%	17%	48%
Cladding heat capacity	6%	15%	19%	20%	20%	7%	9%	7%	6%	9%	14%
Cladding elastic modulus	10%	9%	9%	11%	11%	9%	7%	13%	17%	10%	13%
Cladding corrosion model during steady-state operation	10%	11%	29%	22%	22%	100%	100%	21%	57%	15%	11%
Cladding hydrogen pickup fraction during steady-state operation	11%	10%	10%	7%	7%	11%	6%	10%	6%	11%	11%
Cladding oxidation model at high temperature	13%	7%	7%	18%	18%	83%	84%	10%	11%	11%	4%
Thermal conductivity of the oxide layer	6%	5%	5%	10%	10%	8%	8%	7%	7%	6%	6%
Fission gas release (or gas diffusion coefficient)	8%	5%	7%	6%	10%	9%	9%	9%	13%	9%	2%
Gap gas conductivity	17%	59%	91%	48%	47%	15%	17%	47%	14%	19%	44%
Fuel/cladding emissivity	8%	7%	19%	13%	13%	9%	7%	17%	11%	10%	10%
Fuel radial relocation	10%	6%	8%	17%	15%	8%	8%	6%	7%	7%	8%
Fuel fragment packing fraction (if applicable)	14%	7%	7%	10%	10%	12%	12%	8%	6%	12%	11%
Cladding strain threshold for fuel mobility (if applicable)	12%	4%	5%	15%	15%	15%	13%	8%	10%	15%	8%
Cladding Meyer hardness	8%	11%	11%	16%	16%	9%	9%	13%	12%	7%	4%
Cladding annealing	65%	51%	79%	82%	82%	28%	56%	90%	47%	63%	35%
Cladding burst criteria	9%	4%	9%	5%	5%	7%	5%	14%	9%	10%	6%
Cladding burst strain criteria	6%	10%	9%	10%	9%	5%	12%	10%	11%	6%	5%
Plenum gas temperature [°C]	95%	5%	16%	23%	23%	9%	13%	21%	88%	15%	12%

Tab 3: High influential input uncertainty parameters based on PRCC at their maximum for each output from one participant.

Input uncertainty parameter	Fuel Thermal +RIP	Clad thermal +ECR	Fuel/Clad Mechanical	Overall
Cladding outside diameter (mm)	0	1	1	1
Cladding inside diameter (mm)	1	1	1	1
Pellet outside diameter	1	1	1	1
Fuel theoretical density (kg/m3 at 20 °C)	0	0	0	0
U235 enrichment (%)	0	0	0	0
Filing gas pressure (MPa)	1	0	1	1
Relative power during base irradiation	0	0	0	0
Relative power during test	1	1	1	1
Test rod power profile	0	0	1	1
Cladding temperature (°C)	1	1	1	1
Coolant temperature (°C)	1	1	1	1
Clad-to-Coolant heat transfer coefficient	1	1	1	1
Fuel thermal conductivity model	1	0	1	1
Clad thermal conductivity model	0	1	0	1
Fuel thermal expansion model	1	0	1	1
Clad thermal expansion model	1	0	1	1
Fuel densification model	0	0	1	1
Fuel solid swelling model	0	0	1	1
Fuel gaseous swelling model	0	0	1	1
Clad Yield stress	1	1	1	1
Fuel heat capacity	1	1	0	1
Cladding heat capacity	0	0	0	0
Cladding elastic modulus	0	0	1	1
Cladding corrosion model during steady-state operation	0	1	1	1
Cladding hydrogen pickup fraction during steady-state operation	0	0	0	0
Cladding oxidation model at high temperature	0	1	0	1
Thermal conductivity of the oxide layer	0	0	0	0
Fission gas release (or gas diffusion coefficient)	0	0	0	0
Gap gas conductivity	1	1	1	1
Fuel/cladding emissivity	0	0	0	0
Fuel radial relocation	0	0	0	0
Fuel fragment packing fraction (if applicable)	0	0	0	0
Cladding strain threshold for fuel mobility (if applicable)	0	0	0	0
Cladding Meyer hardness	0	0	0	0
Cladding annealing	1	1	1	1
Cladding burst criteria	0	0	0	0
Cladding burst strain criteria	0	0	0	0
Plenum gas temperature [°C]	1	0	1	1

Tab 4: Common list of high influential input uncertainty parameters for each fuel modelling aspect.

In summary, the following input uncertainty parameters are of high influence on the overall fuel code models, including fuel and cladding thermal and mechanical modelling:

- Fuel rod geometry (clad outside/inside diameter, fuel pellet diameter);
- Test conditions: filling gas pressure, power and clad-to-coolant heat transfer (coolant temperature and clad-to-coolant heat transfer coefficients, or clad temperature) during the test. The axial power profile is also important for mechanical modelling;
- Material properties and models related to fuel-to-clad heat transfer (including fuel thermal conductivity and heat capacity, gap conductivity); fuel thermal expansion, densification and swelling; cladding thermal expansion, Yield stress, annealing; cladding steady-state corrosion and high-temperature oxidation;
- Plenum gas temperature.

On the contrary, the following input uncertainty parameters appear to have only low or medium influence:

- Fuel manufacturing data (Fuel density, Enrichment);
- Operation conditions: Relative power during base irradiation;
- Material properties and models related to clad heat capacity and Mayer hardness, burst strain criteria or burst stress and strain criteria; Fuel radial relocation, fuel/cladding emissivity, fission gas release. The axial relocation related parameters (fuel fragmentation fraction, Strain threshold for fuel mobility) have no influence as the axial relocation model is not used.

The non-significance of some input uncertainty parameters is surprising. For example, in FRAPTRAN (without the axial relocation model), the ballooning and burst are predicted by the BALON2 model which calculates the extent and shape of the localized large cladding deformation (ballooning) that occurs between the time that the cladding effective strain exceeds the instability strain and the time of cladding rupture. In particular, the BALON2 model predicts failure (burst) in the ballooning node when the cladding true hoop stress exceeds an empirical limit that is a function of cladding temperature, or when the predicted cladding permanent hoop strain exceeds the strain limit that is a function of cladding temperature. It is expected that there should be at least an impact of the "cladding burst stress criteria" or "cladding burst strain criteria".

However, we must not forget the limitations of using the correlation coefficients. Indeed, the impact of a single input uncertainty parameter on a specific output parameter could be non-linear and non-monotonic and thus not captured by the correlation coefficients like PRCC. Another explanation would be that those parameters affect only the burst time, but not the other parameters. This would make their effect harder to notice. Additional efforts would be necessary to investigate those questions by plotting and displaying flyspecks or extracting and studying the burst instants. An alternative approach is to use other sensitivity indices such as Sobol's [11].

6. Conclusions and perspectives

Within the framework of the IAEA FUMAC project, an uncertainty and sensitivity analysis has been performed on the simulation of the Halden LOCA test IFA-650.10, according to detailed Specifications. Seven participated have submitted their uncertainty analysis results, and six participated have submitted their sensitivity analysis results. The provided results were compared and discussed, in comparison with the available experimental data.

The comparison of the uncertainty analysis shows that the uncertainty bands (i.e., difference between the lower and upper bound values) are acceptable for the fuel and clad thermal behaviour (RIP, TCO and TFO), but quite large for the clad mechanical behaviour prediction (ECT and DCO). The mechanical models for the clad deformation still need to be improved, at least for certain fuel rod codes (i.e., FRAPTRAN). It is even more important that the initial uncertainty on the failure criteria considered in this work is certainly underestimated when compared to the experimental data on which the criterion is built.

The comparison of the sensitivity analysis results helps to identify a common list of high influential input uncertainty parameters for each output parameter, and for each aspect (fuel and clad thermal and mechanical modelling) and overall models of the fuel rod code.

It should be noted that there exists a significant user effect, as illustrated by the differences in the three results of FRAPTRAN calculations.

Acknowledgments

This work was performed within the IAEA Coordinated Research Project on Fuel Modeling in Accident Conditions (CRP T12028).
The authors would like to acknowledge the contribution of A. SOBA (CNEA), C. STRUZIK (CEA), S. CHEN (CIAE), L. E. HERRANZ (CIEMAT), A. ABE (IPEN), P. VAN UFFELEN and A. SCHUBERT (JRC), A. DETHIOUX and T. DRIEU (Tractebel), who performed the analysis and provided the results, and W. WIESENACK (HRP) who provided the IFA650.10 test data.
J. Zhang is also grateful to Engie Nuclear Development Division (DDN) for supporting Tractebel's participation in the FUMAC project, and to Dr. L. O. JERNKVIST for proving the support in the improvement of the FRAPTRAN-TE-1.5 code.

7. References

[1] M. Veshchunov, J. Stuckert, P. Van Uffelen, W. Wiesenack, J. Zhang, "FUMAC: IAEA's Coordinated Research Project on Fuel Modelling in Accident Conditions," Trans. TopFuel 2018, Prague, Czech Republic, 30 September – 4 October 2018, ENS (2018).

[2] INTERNATIONAL ATOMIC ENERGY AGENCY, Improvement of computer codes used for fuel behaviour simulation (FUMEX-III). IAEA-TECDOC-1697, IAEA, Vienna (2013).

[3] A. Lavoil, "LOCA Testing at Halden, the Tenth Experiment IFA-650.10", HWR-974, OECD Halden Reactor Project, December 2010.

[4] J. Zhang, J. Segurado and Ch. Schneidesch, "Towards an Industrial Application of Statistical Uncertainty Analysis Method to Multi-physical Modelling and Safety Analyses," OECD/CSNI Workshop on Best Estimate Methods and Uncertainty Evaluations, Barcelona, Spain, 16-18 November, 2011.

[5] E. Gentle, "Monte-Carlo Methods," Encyclopaedia of Statistics, 5, pp. 612-617, John Wiley and Sons, New-York, 1985.

[6] W. Conover, Practical non-parametric statistic, Wiley, New York, 1999.

[7] S.S. Wilks, Determination of sample sizes for setting tolerance limits, Ann. Math. Stat. 12, 91–96, 1941.

[8] A. Guba, M. Makai, L. Pal: "Statistical aspects of best estimate method-I"; Reliability Engineering and System Safety 80, 217-232, 2003.

[9] M. D. McKay, "Sensitivity and uncertainty analysis using a statistical sample of input values," Ch. 4, Uncertainty Analysis, Ronen, Y. Editor, CRC Press, Florida, USA, 1988.

[10] J.C. Helton, J.D. Johnson, C.J. Sallaberry, C.B. Storlie, "Survey of sampling-based methods for uncertainty and sensitivity analysis," Reliability Engineering and System Safety, 91(10), 10/2006.

[11] B. looss and P. Lemaitre, "A review on global sensitivity analysis methods," in Uncertainty management in Simulation-Optimization of Complex Systems: Algorithms and Applications (C. Meloni and G. Dellino, Eds), Springer, 2015, http://www.springer.com/business.